

## **Simultaneous shaping and confinement of metal-organic polyhedra in alginate-SiO<sub>2</sub> spheres**

Zhuxiu Zhang,<sup>a</sup> Yifan Lei,<sup>a</sup> Jie Zhou,<sup>a</sup> Mifen Cui,<sup>a</sup> Xian Chen,<sup>a</sup> Zhaoyang Fei,<sup>a</sup> Qing Liu,<sup>a</sup> Jihai Tang,<sup>\*,a,b</sup> and Xu Qiao<sup>\*,a,b</sup>

<sup>a</sup>State Key Laboratory of Materials-Oriented Chemical Engineering, College of Chemical Engineering, Nanjing Tech University, No. 30 Puzhunan Road, Nanjing 211816, China.

<sup>b</sup>Jiangsu National Synergetic Innovation Centre for Advanced Materials (SICAM), No. 5 Xinmofan Road, Nanjing 210009, China.

## **Material**

All reagents and solvents were purchased from commercial sources and used without further purification.

### **Synthesis of Cu-MOP**

$\text{Cu}(\text{NO}_3)_2$  (483 mg) and isophthalic acid (332 mg) were dissolved in methanol (20 mL). Then 465  $\mu\text{L}$  2,6-lutidine was added into the mixture and reacted for 12 h. The Cu-MOP crystallite was obtained after filtration and vacuum drying at 60 °C for 8 h.

### **Synthesis of MOP-alginate**

The dripping of alginate aqueous solution (2 wt%, 10 mL) in the solution of  $\text{Cu}(\text{NO}_3)_2$  (0.24 mol/L, 20 mL) afforded sphere-like hydrogel (Cu-alginate). The obtained Cu-alginate was transferred to methanol solution of isophthalic acid. The mixture was allowed to stand at room temperature for 12 h after adding two drops of 2,6-lutidine. MOP-alginate was then obtained and washed with methanol several times.

### **Synthesis of Cu-alginate-SiO<sub>2</sub>**

The dripping of alginate aqueous solution (2 wt%, 10 mL) in the solution of  $\text{Cu}(\text{NO}_3)_2$  (0.24 mol/L, 20 mL) afforded sphere-like hydrogel (Cu-alginate). The obtained Cu-alginate was transferred to ethanol solution of ethyl orthosilicate (volume ratio 1:1) and reacted for 24 h. The afforded sphere-like hydrogel was added into deionized water and stirred for 2 h. Cu-alginate-SiO<sub>2</sub> was then obtained and washed with methanol several times.

### **Synthesis of MOP-alginate-SiO<sub>2</sub>**

The prepared Cu-alginate hydrogel was soaked in the 10 mL mixture solution (tetraethoxysilane:methanol = 1:1) overnight. Then the hydrogel was isolated and dispersed in deionized water for 2 hours followed by being washed with water and methanol. The obtained Cu-alginate-SiO<sub>2</sub> was transferred to methanol solution of 1,3-bdc. The mixture was allowed to stand at room temperature for 12 h after adding two

drops of 2,6-lutidine. MOP-alginate-SiO<sub>2</sub> was obtained and washed with methanol several times. The MOP-alginate-SiO<sub>2</sub> based upon the derivatives of prototypal MOP were synthesized according to this procedure. We used 5-OH-1,3-bdc, 5-NH<sub>2</sub>-1,3-bdc, 5-CH<sub>3</sub>-1,3-bdc and 5-Br-1,3-bdc respectively to synthesize MOP-OH-alginate-SiO<sub>2</sub>, MOP-NH<sub>2</sub>-alginate-SiO<sub>2</sub>, MOP-CH<sub>3</sub>-alginate-SiO<sub>2</sub> and MOP-Br-alginate-SiO<sub>2</sub>.

### **Characterizations**

UV-vis spectra were collected on the PerkinElmer Lambda 35 in the region of 200-800 nm. Powder X-ray diffraction (XRD) patterns of the samples were collected at 40 kV and 40 mA on a Rigaku SmartLab diffractometer with Cu K $\alpha$  ( $\lambda = 1.5416 \text{ \AA}$ ) radiation. MALDI-TOF mass spectra were recorded on a Bruker UltrafleXtreme using DCTB as a matrix. Transmission electron microscopy (TEM), high-angle annular dark-field scanning TEM (HAADF-STEM) and element mapping analysis were obtained on a FEI F30 electron microscope at 200 kV. <sup>1</sup>H and <sup>13</sup>C NMR spectra were measured on a Bruker 400 MHz (400 MHz for <sup>1</sup>H, 100 MHz for <sup>13</sup>C) spectrometer at room temperature. Fourier transform infrared (FT-IR) spectra were performed on a Thermo-Nicolet AVATAR 360 IR spectrometer over the range of 500 cm<sup>-1</sup> to 4000 cm<sup>-1</sup> with a KBr detector at room temperature. The ICP-OES analysis was conducted on the Perkin Elmer Optima7000DV. Gas sorption isotherms of MOP-alginate-SiO<sub>2</sub> was collected using the 3Flex sorption instrument. Before measurements, freshly prepared samples were soaked with methanol, followed by being activated using the supercritical CO<sub>2</sub> in a Tousmimis Samdri PVT-3D critical point dryer. N<sub>2</sub> sorption isotherms were collected at 77 K using liquid N<sub>2</sub> bath. Compression testing of samples with cylinder shape were carried out via electronic tension testing machine (MZ-2000C) with a rate of 10 mm/min at room temperature.

### **Calculation of MOP loading**

The MOP content  $\omega_4$  and the proportion of MOP/(MOP+alginate)  $\omega_5$  in the MOP-alginate-SiO<sub>2</sub> was calculated based upon the thermogravimetric analysis (TGA) under oxygen atmosphere from 30-800 °C at the ramping of 10 °C/min on a TGA/DSC3+ instrument. The calculation equation is as follows:

$$\omega_4 = \frac{M_1 \times \left( \omega_1 - \frac{\omega_1}{\omega_2} \left( 1 - \frac{1 - \omega_2}{1 - \omega_3} \right) \right)}{24 \times M_2} \times 100\% \quad (1)$$

$$\omega_5 = \frac{M_1 \times \left( \omega_1 - \frac{\omega_1}{\omega_2} \left( 1 - \frac{1 - \omega_2}{1 - \omega_3} \right) \right)}{24 \times M_2 \times \left( 1 - \frac{\omega_1}{\omega_2} \left( 1 - \frac{1 - \omega_2}{1 - \omega_3} \right) \right)} \times 100\% \quad (2)$$

Where  $\omega_4$  is the weight percent of MOP in MOP-alginate-SiO<sub>2</sub>;  $\omega_5$  is the proportion of MOP/(MOP+alginate) in MOP-alginate-SiO<sub>2</sub>;  $\omega_1$  is the weight percent of CuO and SiO<sub>2</sub> in MOP-alginate-SiO<sub>2</sub>;  $\omega_2$  is the weight percent of CuO and SiO<sub>2</sub> in Cu-alginate-SiO<sub>2</sub>;  $\omega_3$  is the weight percent of CuO in Cu-alginate;  $M_1$  is the molecular weight of MOP;  $M_2$  is the molecular weight of CuO.

The loading of Cu-MOP in MOP-alginate  $\omega_6$  was calculated based on similar method. Where  $\omega_3$  is the weight percent of MOP in MOP-alginate;  $\omega_1$  is the weight percent of CuO in MOP-alginate;  $M_1$  is the molecular weight of MOP;  $M_2$  is the molecular weight of CuO.

$$\omega_6 = \frac{M_1 \times \omega_1}{24 \times M_2} \times 100\% \quad (3)$$

**Table S1** The calculation parameters of Cu-MOP loading

	MOP-alginate-SiO <sub>2</sub>	MOP-alginate
$\omega_1$	62.8%	12.2%
$\omega_2$	68.8%	/
$\omega_3$	21.7%	/
$M_1$	5460.4 g/mol	

$M_2$	79.5 g/mol
-------	------------

The loading of Cu-MOP in MOP-alginate-SiO<sub>2</sub> is 23.2 wt%; the weight ratio between MOP and “MOP+alginate” is 51.6% and the Cu-MOP content in MOP-alginate is 35.1 wt% according to the TGA analysis.

### Catalyst evaluation

Cycloaddition of epoxides with CO<sub>2</sub> was performed in a 10 mL stainless steel autoclave. In a typical procedure, epoxide (20 mmol), tetrabutylammonium bromide (0.3 mmol) and catalyst were transferred into the reactor. In a typical procedure, epoxide (20 mmol), Bu<sub>4</sub>NBr (0.3 mmol) and MOP-alginate-SiO<sub>2</sub> were added to the reactor. For comparison, we also used MOP crystallites, MOP-alginate and Cu-alginate-SiO<sub>2</sub> as catalysts.

- The molar ratio among epoxide, Bu<sub>4</sub>NBr and MOP in MOP-alginate-SiO<sub>2</sub> in the reaction system is: n(epoxide):n(Bu<sub>4</sub>NBr):n(MOP in MOP-alginate-SiO<sub>2</sub>) = 2400:36:1.
- The molar ratio among epoxide, Bu<sub>4</sub>NBr and MOP crystallites is: n(epoxide):n(Bu<sub>4</sub>NBr):n(MOP crystallites) = n(epoxide):n(Bu<sub>4</sub>NBr):n(MOP in MOP-alginate-SiO<sub>2</sub>) = 2400:36:1.
- For MOP-alginate, the alginate in MOP-alginate-SiO<sub>2</sub> is equal to the alginate in MOP-alginate: n(alginate in MOP-alginate-SiO<sub>2</sub>):n(alginate in MOP-alginate) = 1:1.
- The molar ratio among epoxide, Bu<sub>4</sub>NBr and Cu in Cu-alginate-SiO<sub>2</sub> is: n(epoxide):n(Bu<sub>4</sub>NBr):n(Cu in Cu-alginate-SiO<sub>2</sub>) = n(epoxide):n(Bu<sub>4</sub>NBr):n(Cu in MOP-alginate-SiO<sub>2</sub>) = 100:1.5:1.

The reactor was subsequently purged with CO<sub>2</sub> up to 1 MPa at 100 °C. The reaction mixture was collected after three hours and analyzed by gas chromatography equipped with a capillary 30 m × 0.32 mm × 0.25 μm SE-54 column and a flame ionization detector, in which n-butanol was used as the internal standard (Fig. S24-S39). Silica gel column chromatography was used to isolate the target product. The molecular structure of all products were determined by <sup>1</sup>H and <sup>13</sup>C NMR (Fig. S40-S55).

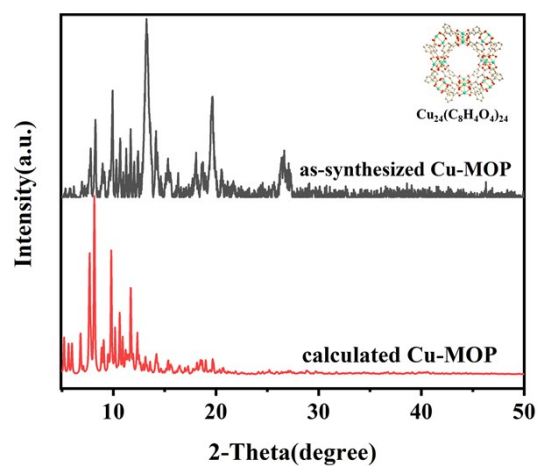


**Figure S1.** PXRD patterns of as-synthesized Cu-MOP and calculated Cu-MOP.

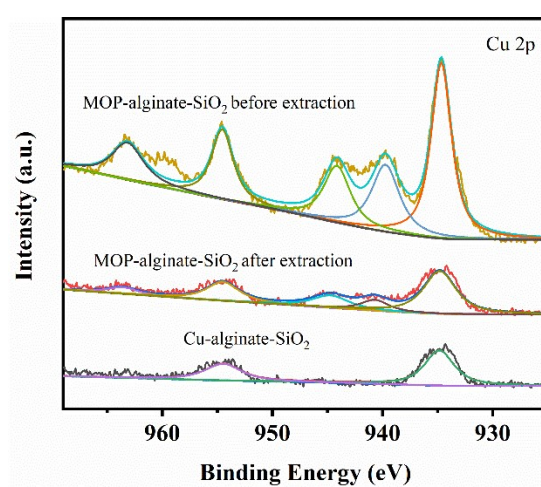


**Figure S2.** XPS spectra of Cu-alginate-SiO<sub>2</sub> and the ball-milled MOP-alginate-SiO<sub>2</sub> powder before and after extraction.

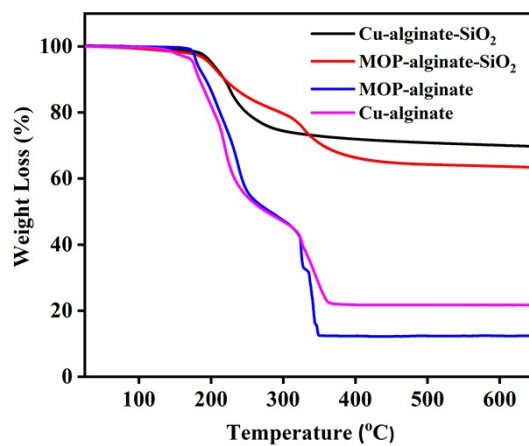


**Figure S3.** TGA curves of Cu-alginate-SiO<sub>2</sub> and MOP-alginate-SiO<sub>2</sub>.

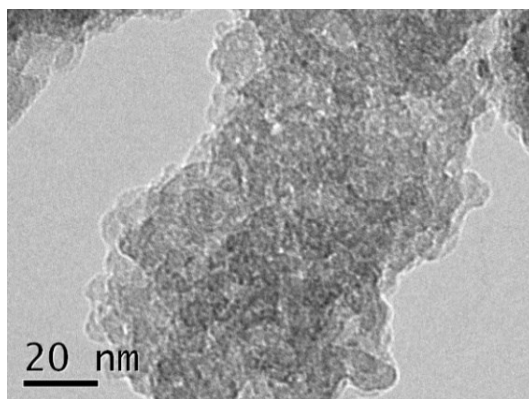


**Figure S4.** TEM image of Cu-alginate-SiO<sub>2</sub>.

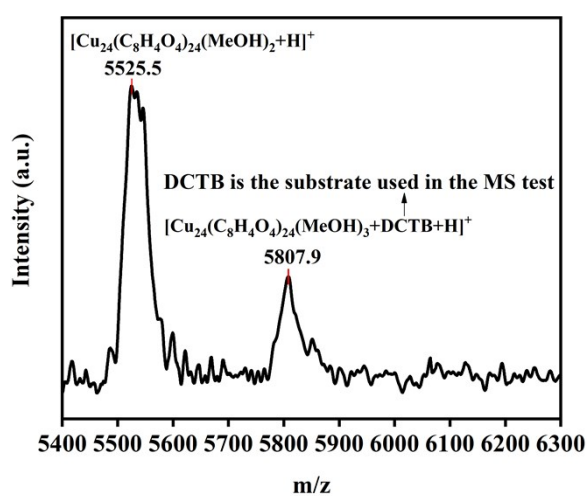


**Figure S5.** MALDI-TOF-MS analysis of Cu-MOP in MOP-alginate.

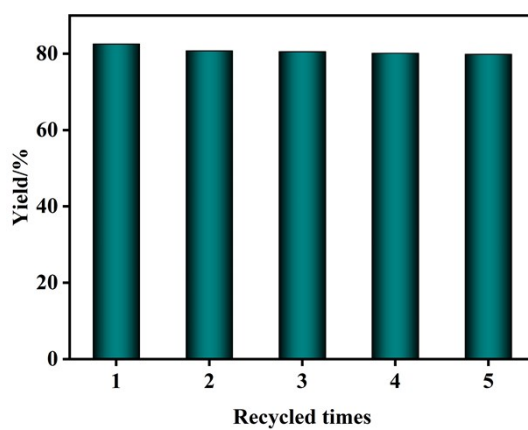


**Figure S6.** Reusability study of MOP-alginate-SiO<sub>2</sub> for CO<sub>2</sub> cycloaddition reaction with propylene oxide.

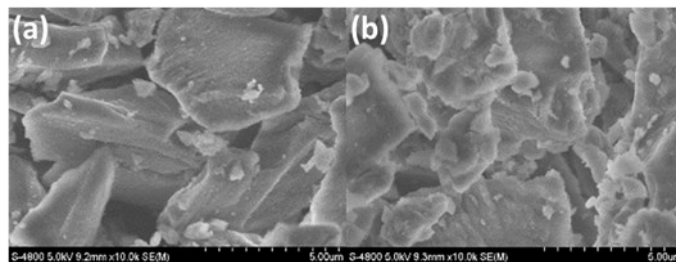


**Figure S7.** SEM images of (a) fresh MOP-alginate-SiO<sub>2</sub> and (b) MOP-alginate-SiO<sub>2</sub> after five cycles.

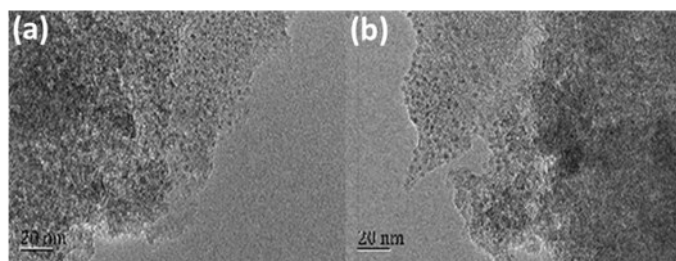


**Figure S8.** TEM images of (a) fresh MOP-alginate-SiO<sub>2</sub> and (b) MOP-alginate-SiO<sub>2</sub> after five cycles.

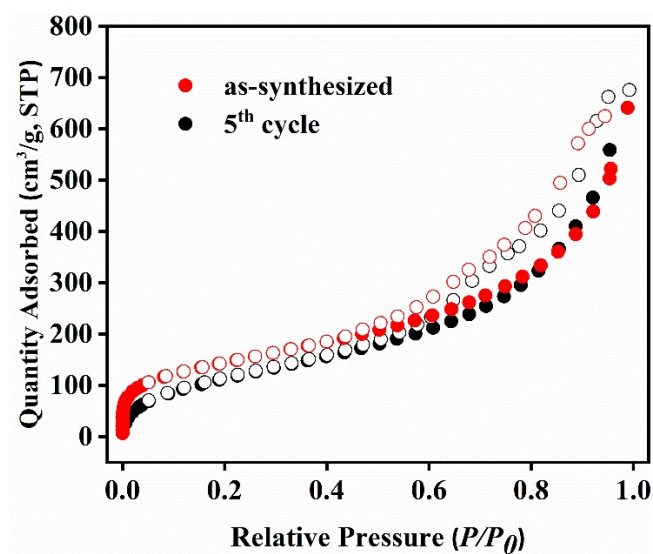


**Figure S9.** N<sub>2</sub> sorption isotherm of as-synthesized MOP-alginate-SiO<sub>2</sub> and MOP-alginate-SiO<sub>2</sub> after five catalytic cycles.

**Determination of the unsaturated Cu sites in MOP-alginate-SiO<sub>2</sub>**



We performed pyridine FT-IR characterization of MOP-alginate-SiO<sub>2</sub> before and after activation to confirm the present of unsaturated Cu sites in Cu-MOP structure (Fig. S11-12). The band at 1069 cm<sup>-1</sup> corresponds to the out-of-plane vibrations of C-C bond when pyridine is adsorbed on the copper paddle wheel.<sup>1</sup> For the activated MOP-alginate-SiO<sub>2</sub>, with the increase of the pyridine amount, the absorbance of the vibration peak at 1069 cm<sup>-1</sup> gradually increased to the maximum absorbance of 1.22, indicating the saturated adsorption of pyridine. In contrast, for the non-activated the MOP-alginate-SiO<sub>2</sub>, the vibration peak at 1069 cm<sup>-1</sup> was not observed after the introduction of pyridine, indicating that all Lewis sites were occupied with solvent molecules instead of pyridine.

In order to quantitatively measure the number of unsaturated Cu sites, we weighed 20 mg sample, compressed it into pellet and introduced small measured doses of pyridine. A series of absorbance corresponding to different pyridine adsorption uptakes were obtained. There was a good linear correlation among these data, and the correlation equation is determined as Absorbance = 1.99 × C<sub>pyridine</sub> with a correlation coefficient of R<sup>2</sup> = 0.999 (Fig S13). According to this equation, at the maximum absorbance of 1.22, the saturated adsorption uptake of pyridine in the MOP-alginate-SiO<sub>2</sub> was 0.61 mmol/g. In Cu-MOP, each unsaturated Cu site only adsorb one pyridine molecule. Therefore, considering the loading of MOP in MOP-alginate-SiO<sub>2</sub> is 23.2 wt%, it could be inferred that one MOP molecule has 14-15 unsaturated Cu sites that could potentially functioned as Lewis acid sites.

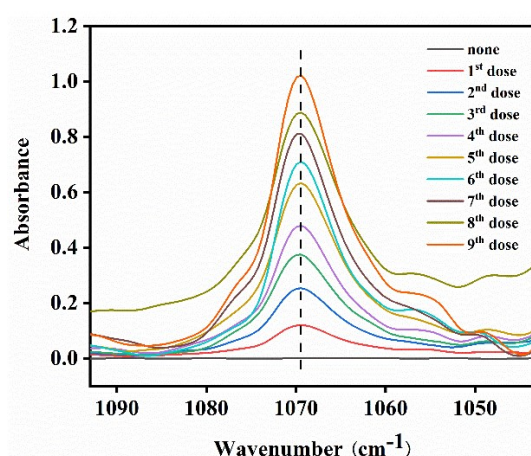


**Fig S10.** IR spectra of quantitative pyridine adsorbed on activated MOP-alginate-SiO<sub>2</sub>.

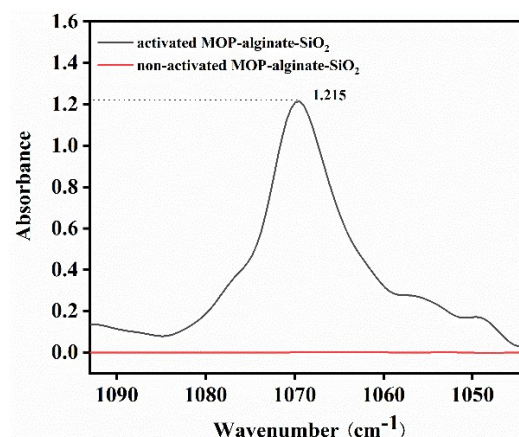


**Fig S11.** IR spectra of pyridine adsorbed on non-activated MOP-alginate-SiO<sub>2</sub> and activated MOP-alginate-SiO<sub>2</sub> with saturated pyridine uptake.

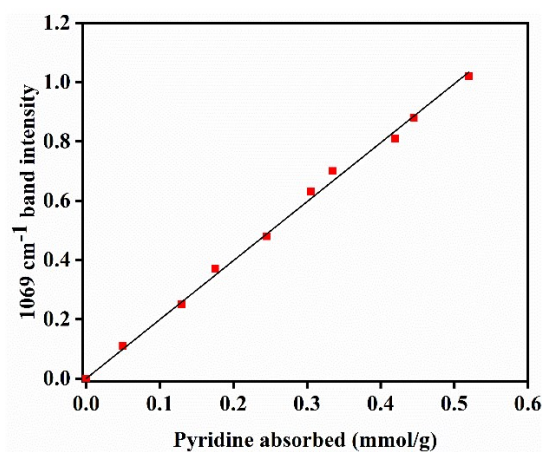


**Fig S12.** Linear correlation between absorbance at 1069 cm<sup>-1</sup> and surface concentration of the adsorbed pyridine.

### Catalyst mechanism

The CO<sub>2</sub> cycloaddition was initialized by the interaction between the unsaturated copper sites and the oxygen from epoxides. Then the less sterically hindered carbon atom of adsorbed epoxides were attacked by the Br<sup>-</sup> nucleophile to form a metal-alkoxide intermediate that subsequently underwent the CO<sub>2</sub> insertion to form corresponding cyclic carbonate.

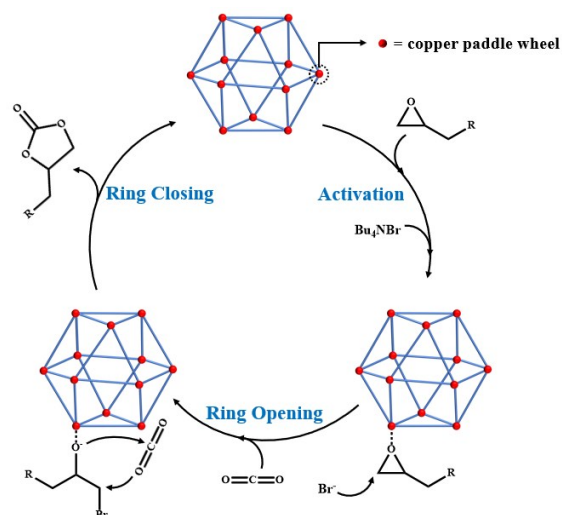


**Figure S13.** Proposed mechanism for the cycloaddition of  $\text{CO}_2$  with epoxides using MOP-alginate- $\text{SiO}_2$  catalysts.

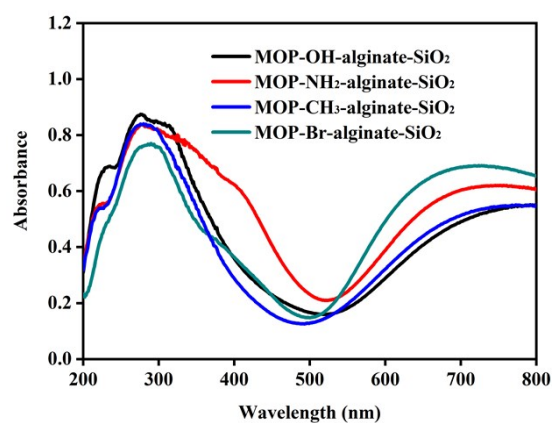


**Figure S14.** UV-vis spectra of MOP-OH/ $\text{NH}_2$ / $\text{CH}_3$ /Br-alginate- $\text{SiO}_2$ .

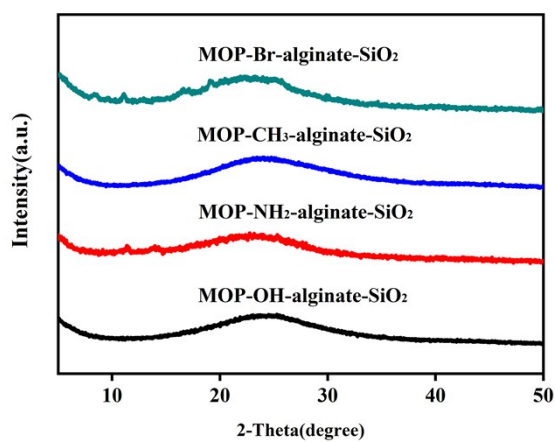


**Figure S15.** PXRD patterns of MOP-Br/ $\text{CH}_3$ / $\text{NH}_2$ / $\text{OH}$ -alginate- $\text{SiO}_2$ .

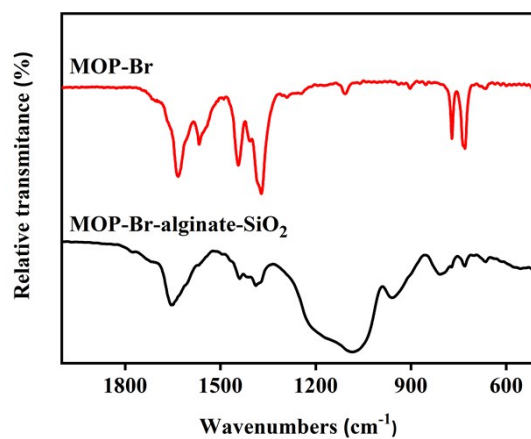


**Figure S16.** FT-IR spectrum of MOP-Br and MOP-Br-alginate-SiO<sub>2</sub>.

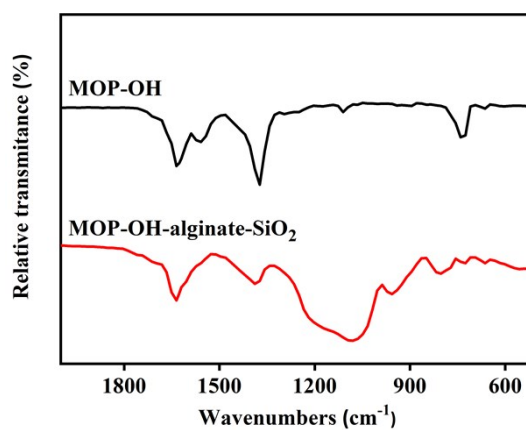


**Figure S17.** FT-IR spectrum of MOP-OH and MOP-OH-alginate-SiO<sub>2</sub>.

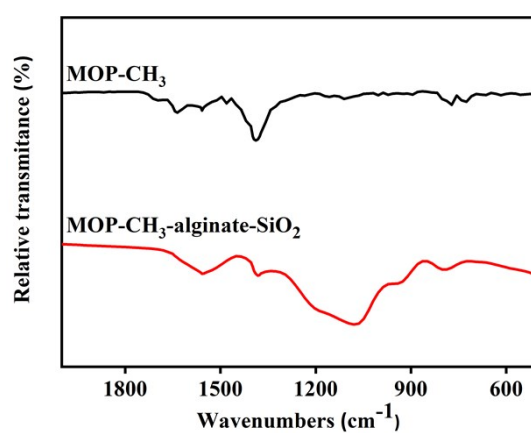


**Figure S18.** FT-IR spectrum of MOP-CH<sub>3</sub> and MOP-CH<sub>3</sub>-alginate-SiO<sub>2</sub>.

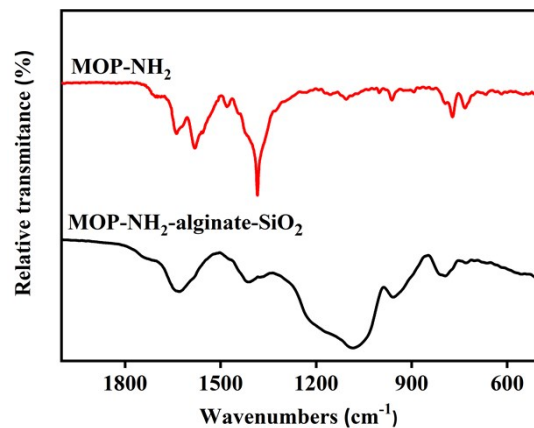


**Figure S19.** FT-IR spectrum of MOP-NH<sub>2</sub> and MOP-NH<sub>2</sub>-alginate-SiO<sub>2</sub>.

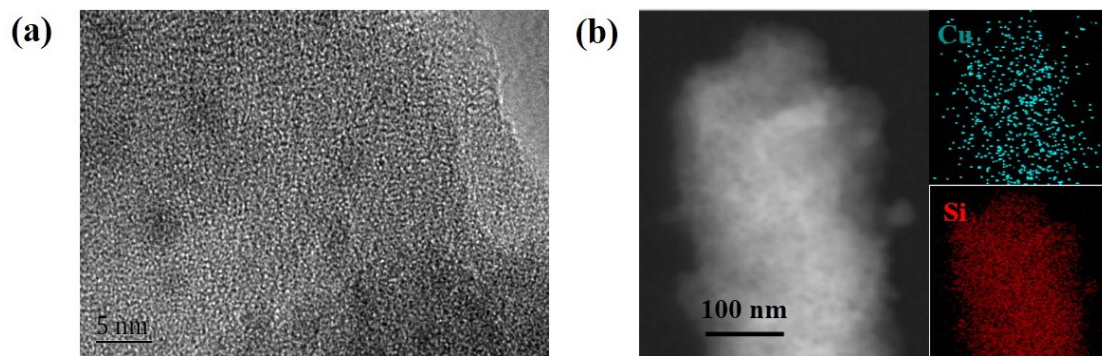


**Figure S20.** (a) TEM image of MOP-OH particles and (b) STEM images MOP-OH-alginate-SiO<sub>2</sub> with corresponding EDX maps of Cu and Si.

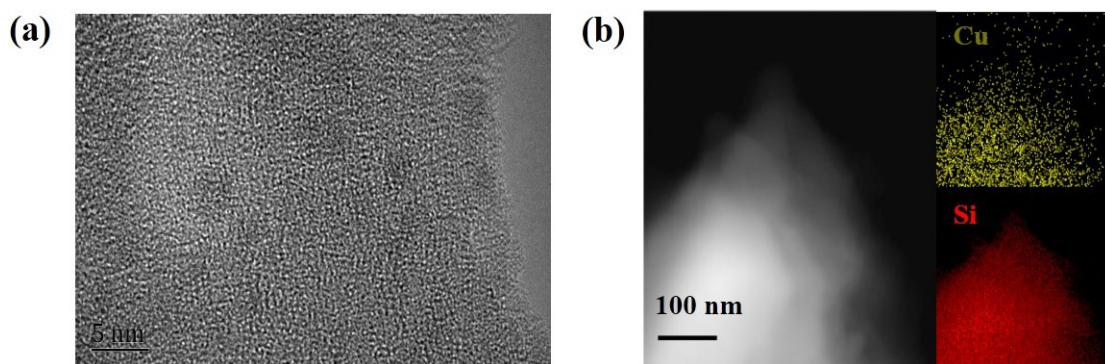


**Figure S21.** (a) TEM image of MOP-NH<sub>2</sub> particles and (b) STEM images MOP-NH<sub>2</sub>-alginate-SiO<sub>2</sub> with corresponding EDX maps of Cu and Si.

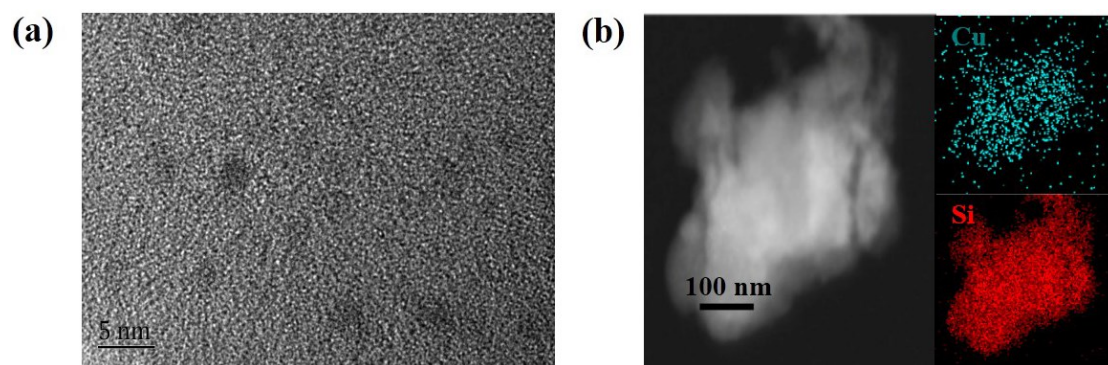


**Figure S22.** (a) TEM image of MOP-CH<sub>3</sub> particles and (b) STEM images MOP-CH<sub>3</sub>-alginate-SiO<sub>2</sub>.with corresponding EDX maps of Cu and Si.

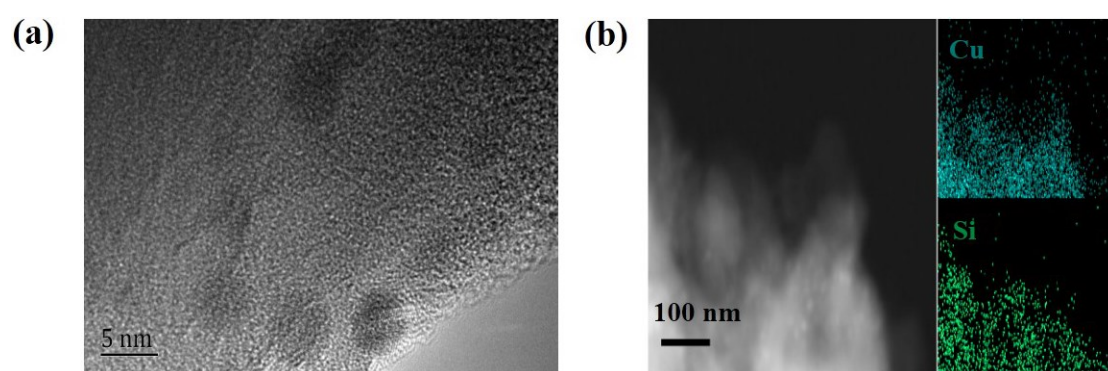
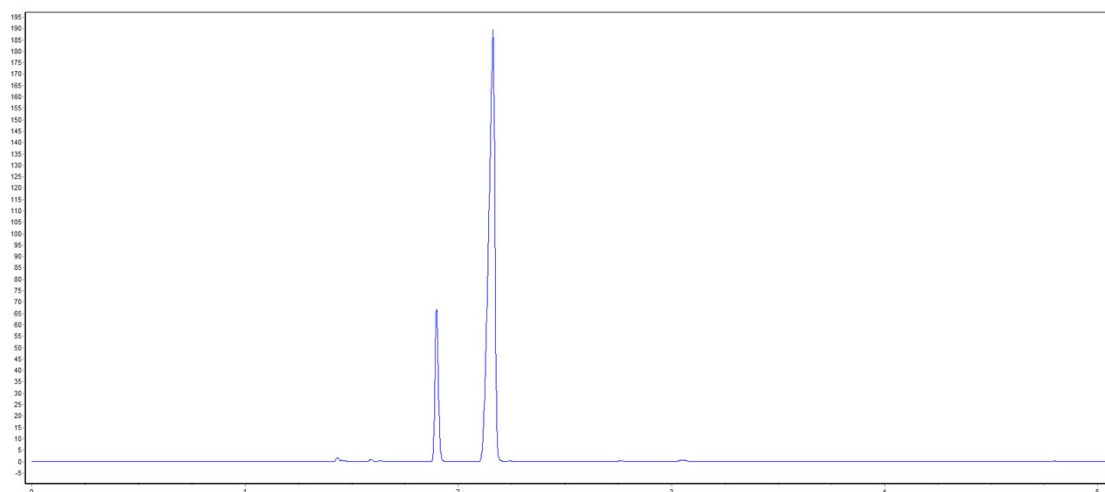


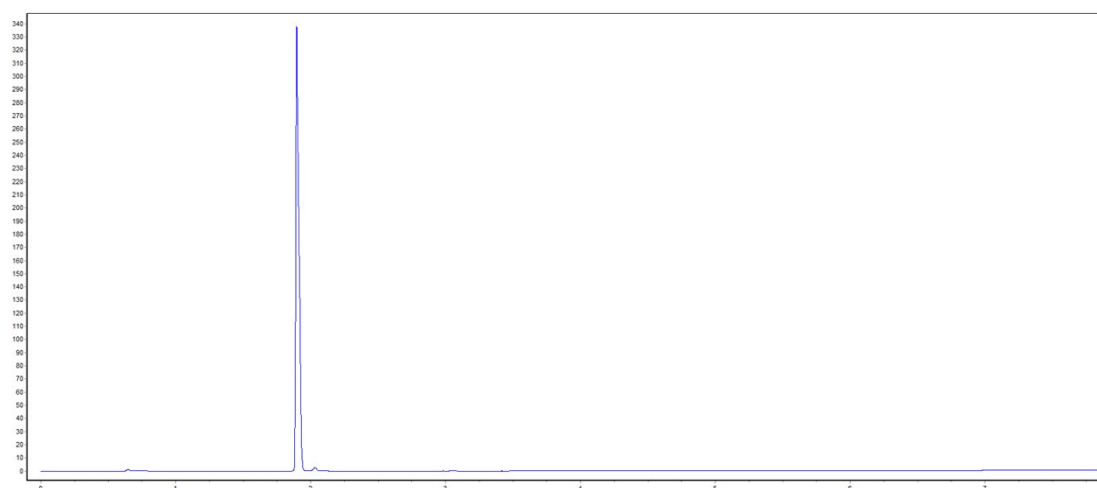
**Figure S23.** (a) TEM image of MOP-Br particles and (b) STEM images MOP-Br-alginate-SiO<sub>2</sub>.with corresponding EDX maps of Cu and Si.



Peak results:

Index	Name	Time [Min]	Quantity [% Area]	Height [mAU]	Area % [%]
1	UNKNOWN	1.87	14.07	66.5	14.073
2	UNKNOWN	2.19	85.93	189.7	85.972
Total			100.00	256.2	100.00

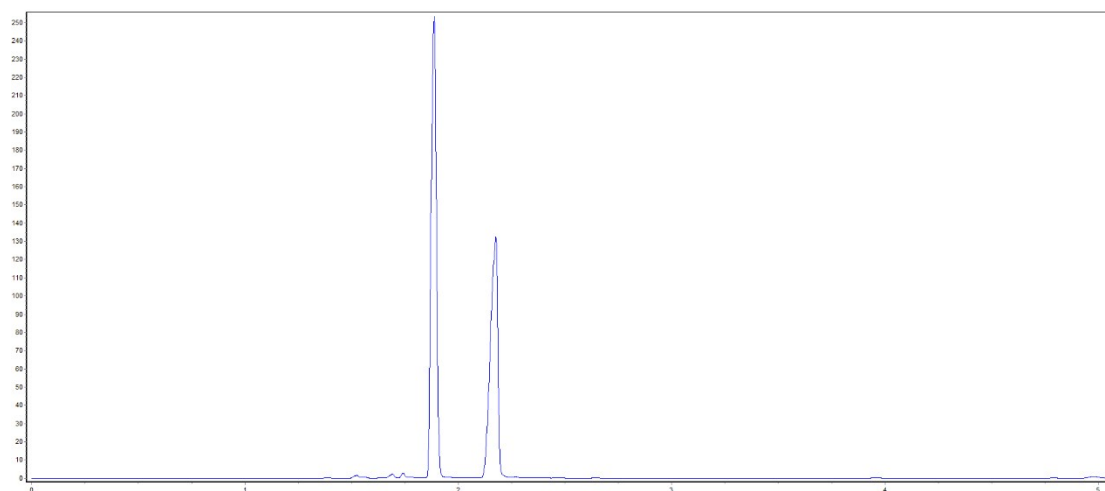
**Figure S24.** Gas chromatogram of the cycloaddition of propylene oxide with CO<sub>2</sub> catalyzed by MOP-alginate-SiO<sub>2</sub> (Table 1, entry 1).



Peak results:

Index	Name	Time [Min]	Quantity [% Area]	Height [mAU]	Area % [%]
1	UNKNOWN	1.87	100.00	336	100.00
Total			100.00	336	100.00

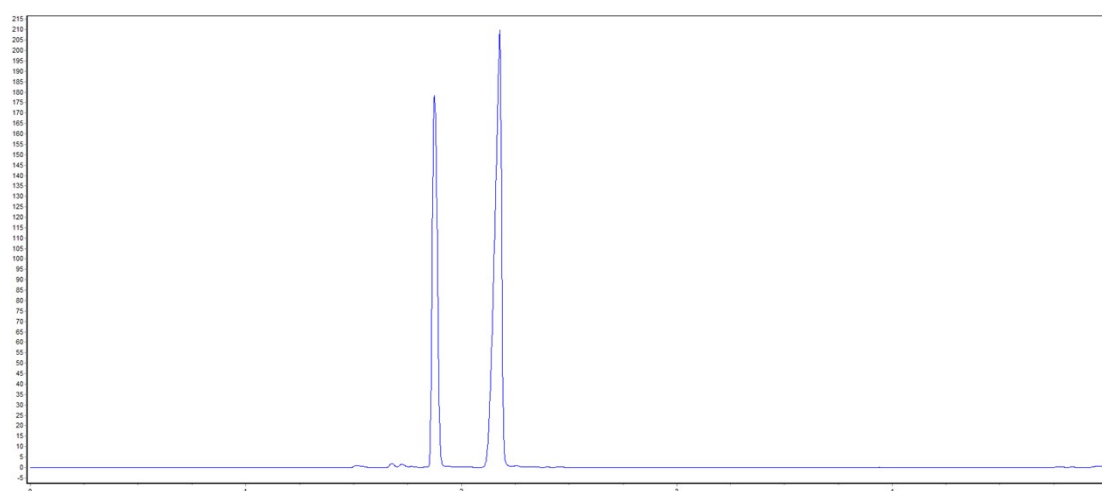
**Figure S25.** Gas chromatogram of the cycloaddition of propylene oxide with CO<sub>2</sub> without catalyst (Table 1 entry 2).



Peak results:

Index	Name	Time [Min]	Quantity [% Area]	Height [mAU]	Area % [%]
1	UNKNOWN	1.89	58.17	251.3	58.168
2	UNKNOWN	2.17	41.83	132.5	41.832
Total			100.00	383.8	100.00

**Figure S26.** Gas chromatogram of the cycloaddition of propylene oxide with CO<sub>2</sub> catalyzed by MOP (Table 1, entry 3).

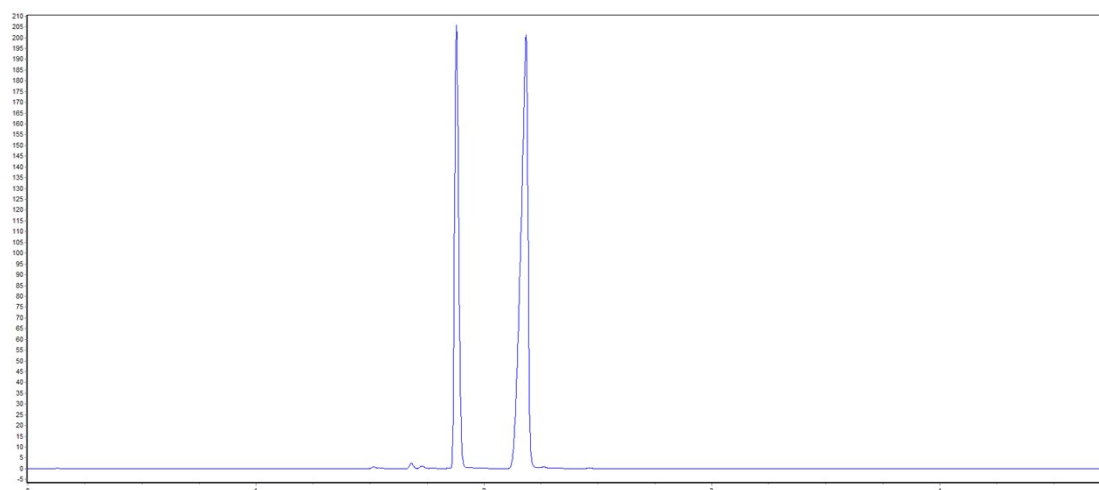


Peak results:

Index	Name	Time [Min]	Quantity [% Area]	Height [mAU]	Area % [%]
1	UNKNOWN	1.87	38.39	177.4	38.393
2	UNKNOWN	2.17	61.61	209.0	61.607
Total			100.00	386.4	100.00

**Figure S27.** Gas chromatogram of the cycloaddition of propylene oxide with CO<sub>2</sub> catalyzed by MOP-alginate (Table 1, entry 4).

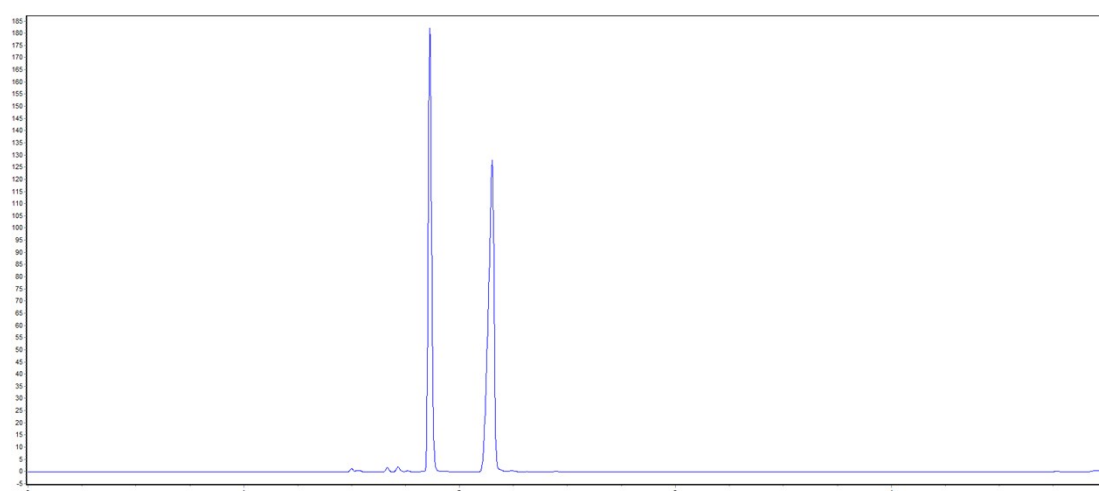




Peak results:

Index	Name	Time [Min]	Quantity [% Area]	Height [mAU]	Area % [%]
1	UNKNOWN	1.88	37.27	204.8	37.274
2	UNKNOWN	2.18	62.73	200.7	62.726
Total			100.00	405.5	100.00

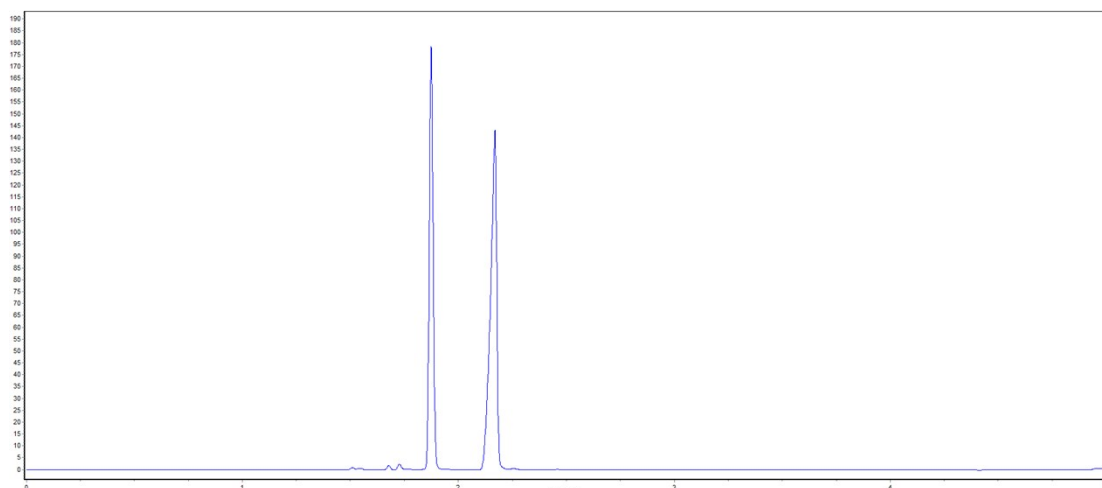
**Figure S28.** Gas chromatogram of the cycloaddition of propylene oxide with CO<sub>2</sub> catalyzed by Cu-alginate-SiO<sub>2</sub> (Table 1, entry 5)



Peak results:

Index	Name	Time [Min]	Quantity [% Area]	Height [mAU]	Area % [%]
1	UNKNOWN	1.86	46.88	180.1	46.883
2	UNKNOWN	2.15	53.12	128.5	53.117
Total			100.00	208.6	100.00

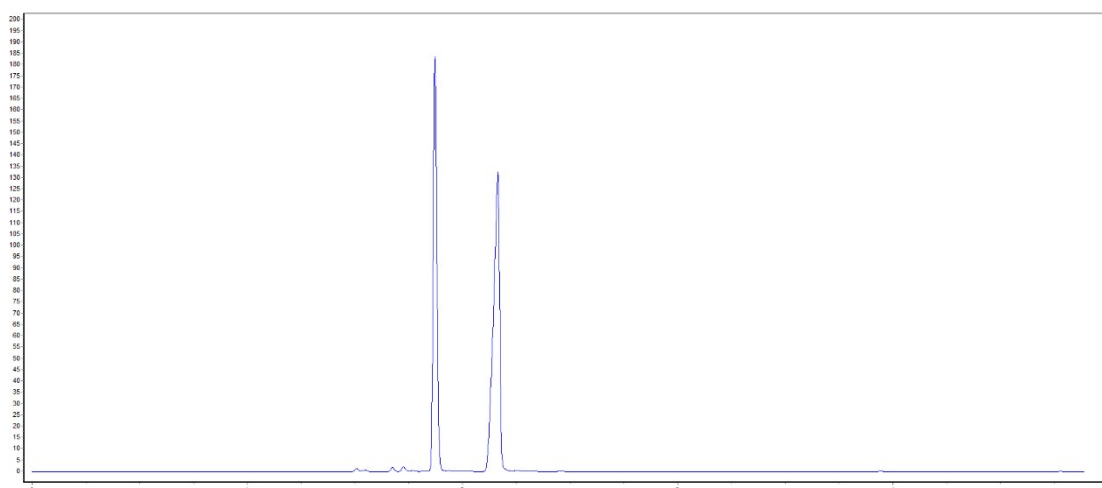
**Figure S29.** Gas chromatogram of the cycloaddition of propylene oxide with CO<sub>2</sub> catalyzed by M3S-0.1 (Table 1, entry 6).



Peak results:

Index	Name	Time [Min]	Quantity [% Area]	Height [mAU]	Area % [%]
1	UNKNOWN	1.87	43.29	179.6	43.289
2	UNKNOWN	2.16	56.71	142.8	56.711
Total			100.00	322.4	100.00

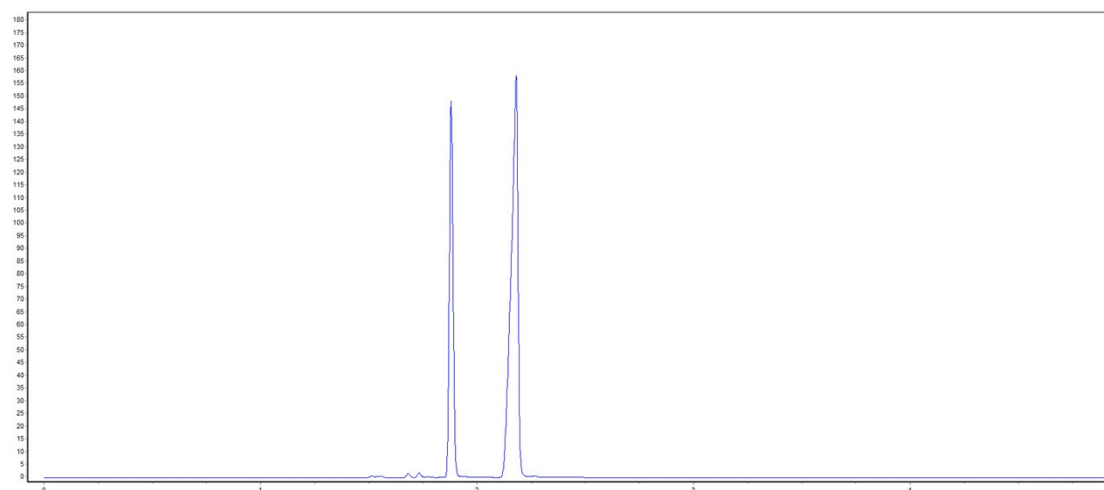
**Figure S30.** Gas chromatogram of the cycloaddition of propylene oxide with CO<sub>2</sub> catalyzed by MOPNT-2 (Table 1, entry 7).



Peak results:

Index	Name	Time [Min]	Quantity [% Area]	Height [mAU]	Area % [%]
1	UNKNOWN	1.87	44.68	179.6	44.684
2	UNKNOWN	2.16	55.32	142.8	55.316
Total			100.00	322.4	100.00

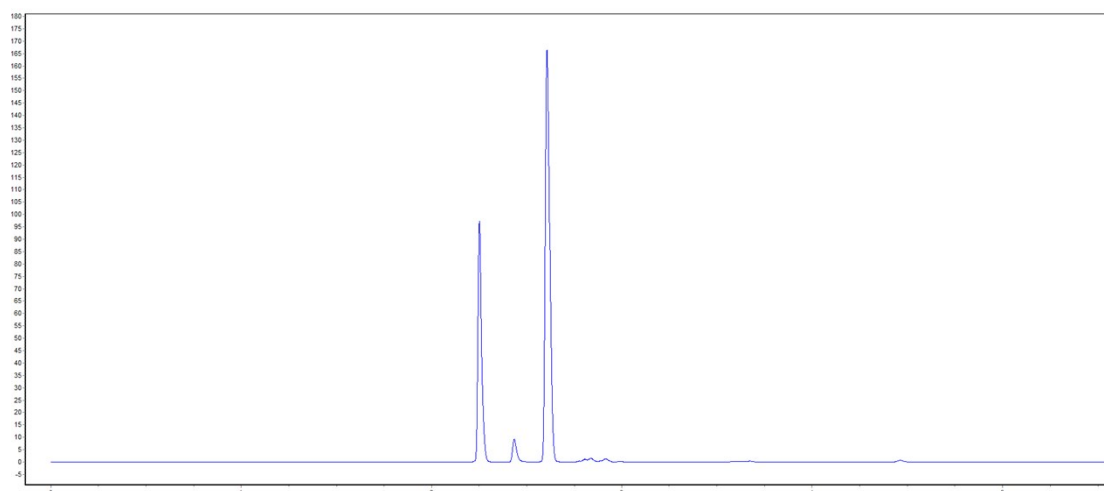
**Figure S31.** Gas chromatogram of the cycloaddition of propylene oxide with CO<sub>2</sub> catalyzed by HKUST-1 (Table 1, entry 8).



Peak results:

Index	Name	Time [Min]	Quantity [% Area]	Height [mAU]	Area % [%]
1	UNKNOWN	1.88	33.46	148.1	33.459
2	UNKNOWN	2.18	66.54	158.2	66.541
Total			100.00	306.3	100.00

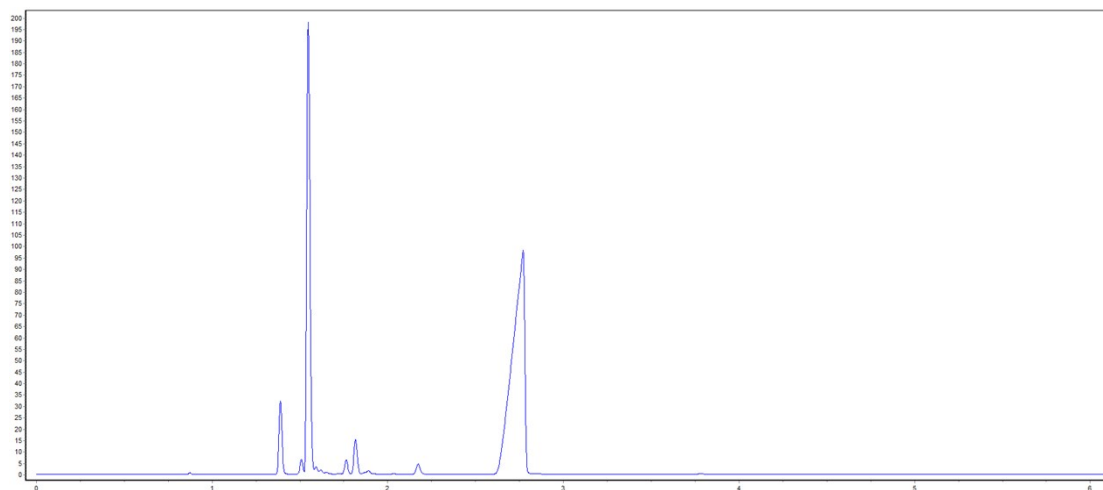
**Figure S32.** Gas chromatogram of the cycloaddition of propylene oxide with CO<sub>2</sub> catalyzed by kagomé (Table 1, entry 9).



Peak results:

Index	Name	Time [Min]	Quantity [% Area]	Height [mAU]	Area % [%]
1	UNKNOWN	2.25	29.79	97.2	29.793
2	UNKNOWN	2.44	3.49	9.3	3.486
3	UNKNOWN	2.60	66.72	166.3	66.721
Total			100.00	272.8	100.00

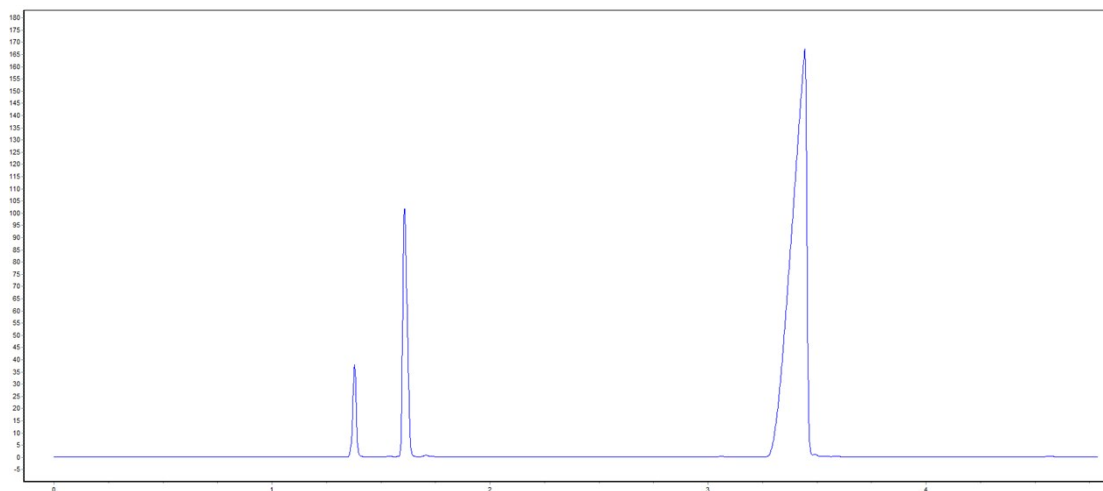
**Figure S33.** Gas chromatogram of the cycloaddition of 2-(trifluoromethyl)oxirane with CO<sub>2</sub> catalyzed by MOP-alginate-SiO<sub>2</sub> (Table 2, entry 1).



Peak results:

Index	Name	Time [Min]	Quantity [% Area]	Height [mAU]	Area % [%]
1	UNKNOWN	1.39	4.50	32.2	4.502
2	UNKNOWN	1.54	34.64	197.4	34.643
3	UNKNOWN	1.76	0.93	6.4	0.926
4	UNKNOWN	1.82	2.37	15.7	2.367
5	UNKNOWN	2.17	0.82	5.0	0.824
6	UNKNOWN	2.77	56.74	97.6	56.738
Total			100.00	354.3	100.00

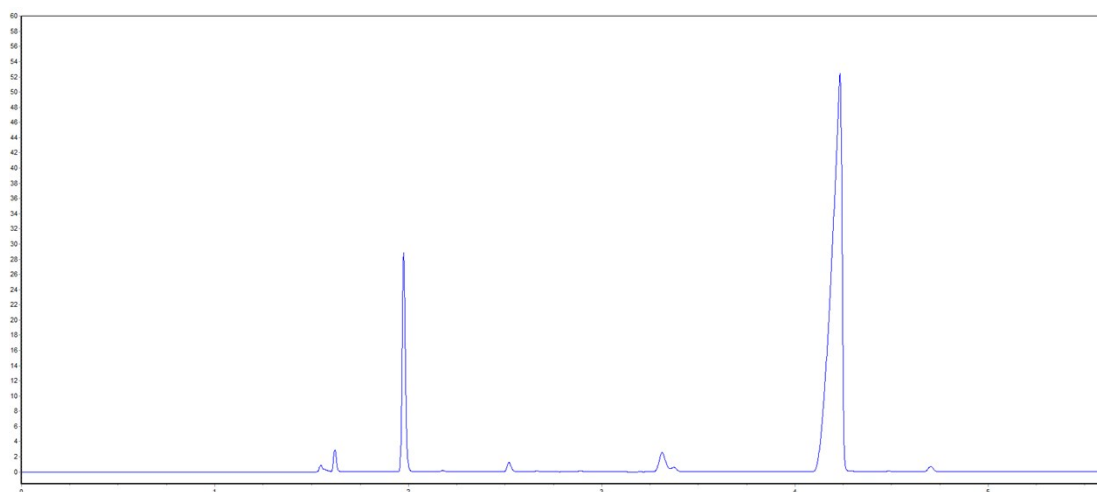
**Figure S34.** Gas chromatogram of the cycloaddition of 2-(chloromethyl)oxirane with CO<sub>2</sub> catalyzed by MOP-alginate-SiO<sub>2</sub> (Table 2, entry 2).



Peak results:

Index	Name	Time [Min]	Quantity [% Area]	Height [mAU]	Area % [%]
1	UNKNOWN	1.38	4.10	38.2	4.103
1	UNKNOWN	1.60	18.71	100.9	18.711
2	UNKNOWN	3.44	77.19	166.2	77.186
Total			100.00	305.3	100.00

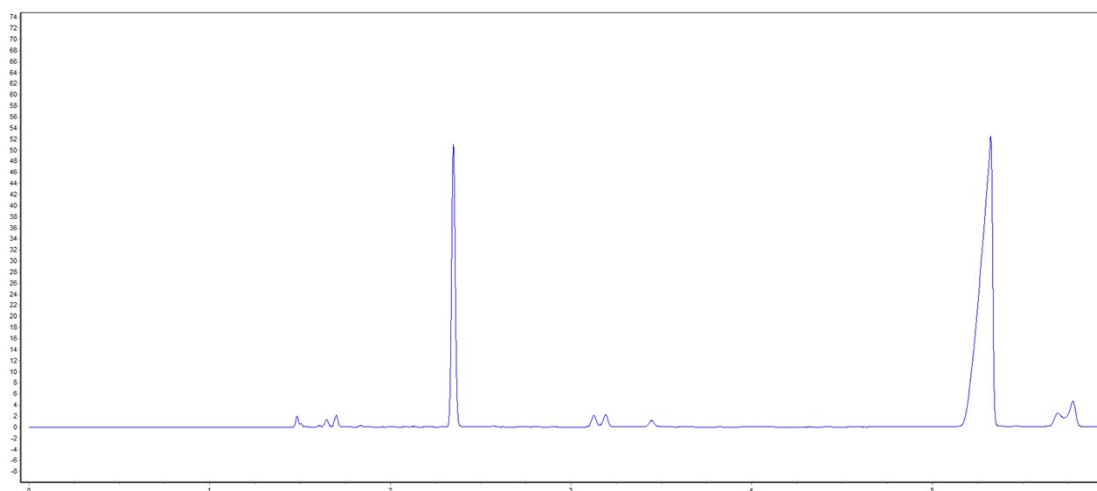
**Figure S35.** Gas chromatogram of the cycloaddition of 2-(but-3-en-1-yl)oxirane with CO<sub>2</sub> catalyzed by MOP-alginate-SiO<sub>2</sub> (Table 2, entry 3).



Peak results:

Index	Name	Time [Min]	Quantity [% Area]	Height [mAU]	Area % [%]
1	UNKNOWN	1.54	0.58	0.9	0.582
2	UNKNOWN	1.62	1.20	2.9	1.195
3	UNKNOWN	1.98	15.51	28.4	15.529
4	UNKNOWN	2.52	0.81	1.2	0.810
5	UNKNOWN	3.31	2.94	2.7	2.937
6	UNKNOWN	4.23	78.43	52.1	78.434
7	UNKNOWN	4.70	0.53	0.7	0.533
Total			100.00	88.9	100.00

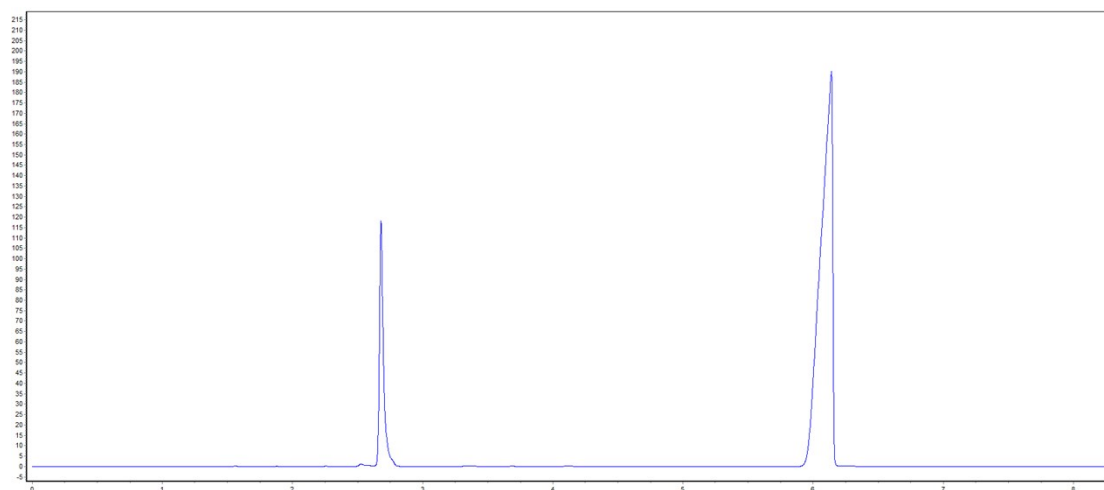
**Figure S36.** Gas chromatogram of the cycloaddition of 2-((allyloxy)methyl)oxirane with CO<sub>2</sub> catalyzed by MOP-alginate-SiO<sub>2</sub> (Table 2, entry 4).



Peak results:

Index	Name	Time [Min]	Quantity [% Area]	Height [mAU]	Area % [%]
1	UNKNOWN	1.49	0.74	2.0	0.743
2	UNKNOWN	1.64	0.61	1.3	0.612
3	UNKNOWN	1.70	0.84	2.1	0.836
4	UNKNOWN	2.34	18.79	50.7	18.788
5	UNKNOWN	3.13	1.20	2.2	1.196
6	UNKNOWN	3.19	1.16	2.2	1.163
7	UNKNOWN	3.44	0.76	1.1	0.764
8	UNKNOWN	5.32	70.67	52.2	70.673
9	UNKNOWN	5.69	2.30	2.5	2.297
10	UNKNOWN	5.78	2.93	4.6	2.928
Total			100.00	120.9	100.00

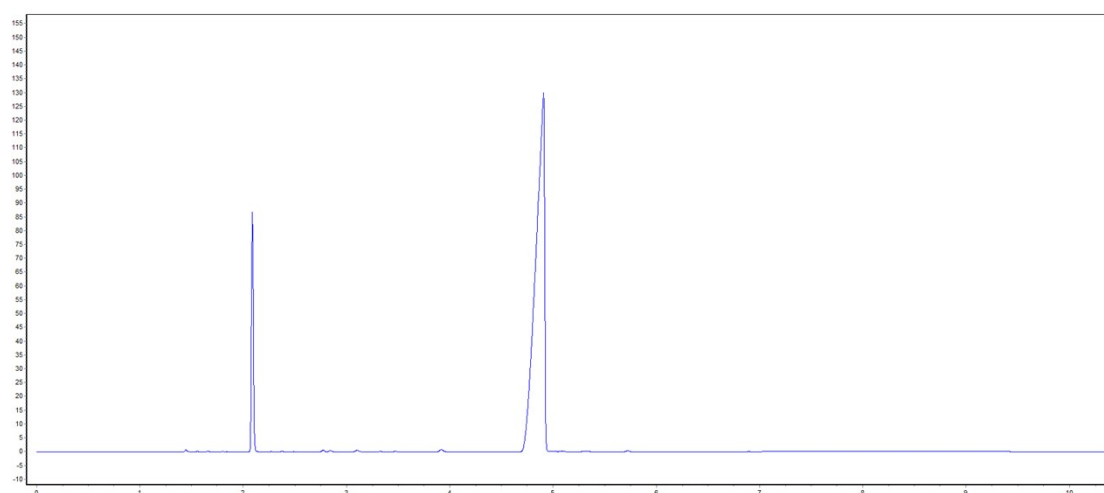
**Figure S37.** Gas chromatogram of the cycloaddition of oxiran-2-ylmethyl methacrylate with CO<sub>2</sub> catalyzed by MOP-alginate-SiO<sub>2</sub> (Table 2, entry 5).



Peak results:

Index	Name	Time [Min]	Quantity [% Area]	Height [mAU]	Area % [%]
1	UNKNOWN	2.67	17.96	117.3	17.963
2	UNKNOWN	6.14	82.04	189.0	82.037
Total			100.00	306.3	100.00

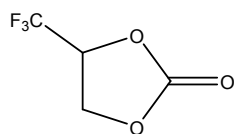
**Figure S38.** Gas chromatogram of the cycloaddition of 2-phenyloxirane with CO<sub>2</sub> catalyzed by MOP-alginate-SiO<sub>2</sub> (Table 2, entry 6).



Peak results:

Index	Name	Time [Min]	Quantity [% Area]	Height [mAU]	Area % [%]
1	UNKNOWN	2.09	15.67	85.8	15.672
2	UNKNOWN	4.92	84.43	129.2	85.428
Total			100.00	215.0	100.00

**Figure S39.** Gas chromatogram of the cycloaddition of 2-(butoxymethyl)oxirane with CO<sub>2</sub> catalyzed by MOP-alginate-SiO<sub>2</sub> (Table 2, entry 7).



**4-(trifluoromethyl)-1,3-dioxolan-2-one**

$^1\text{H}$  NMR (400 MHz,  $\text{DMSO-}d_6$ )  $\delta$  5.61 (dtdd,  $J = 8.2, 6.3, 4.2, 1.6$  Hz, 1H), 4.90 – 4.58 (m, 2H).  $^{13}\text{C}$  NMR (101 MHz,  $\text{DMSO}$ )  $\delta$  153.69, 127.50, 124.71, 121.92, 119.14, 72.48, 72.14, 71.80, 71.46, 64.68.

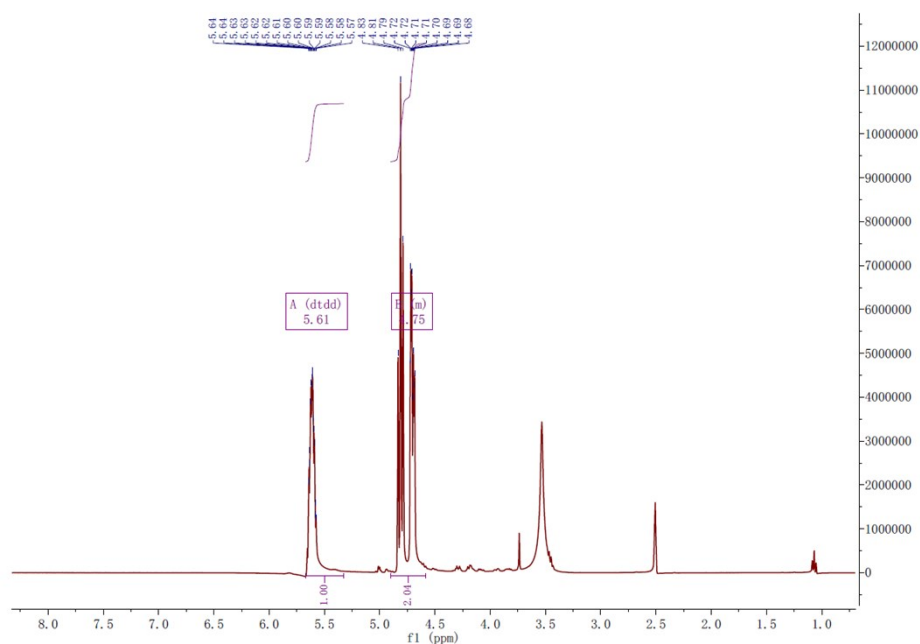


**Figure S40.**  $^1\text{H}$  NMR spectrum of 4-(trifluoromethyl)-1,3-dioxolan-2-one.

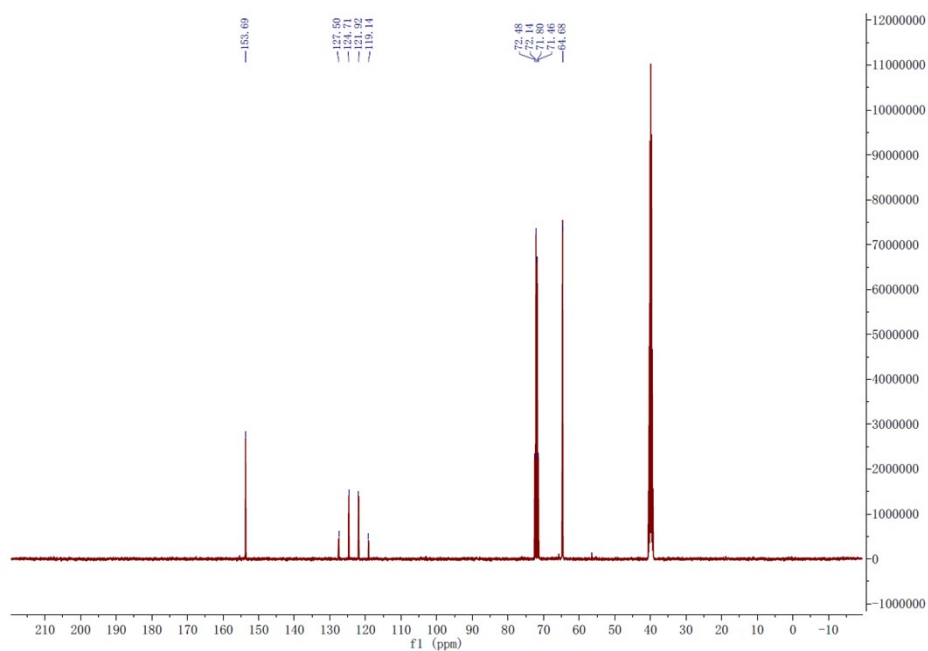
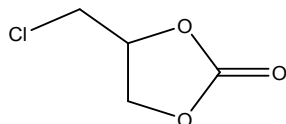


**Figure S41.**  $^{13}\text{C}$  NMR spectrum of 4-(trifluoromethyl)-1,3-dioxolan-2-one.



**4-(chloromethyl)-1,3-dioxolan-2-one**

$^1\text{H}$  NMR (400 MHz,  $\text{DMSO-}d_6$ )  $\delta$  5.12 (dddd,  $J = 8.8, 5.6, 4.2, 3.4$  Hz, 1H), 4.70 – 4.19 (m, 2H), 4.06 – 3.81 (m, 2H).  $^{13}\text{C}$  NMR (101 MHz,  $\text{DMSO}$ )  $\delta$  154.96, 75.39, 67.33, 45.70.

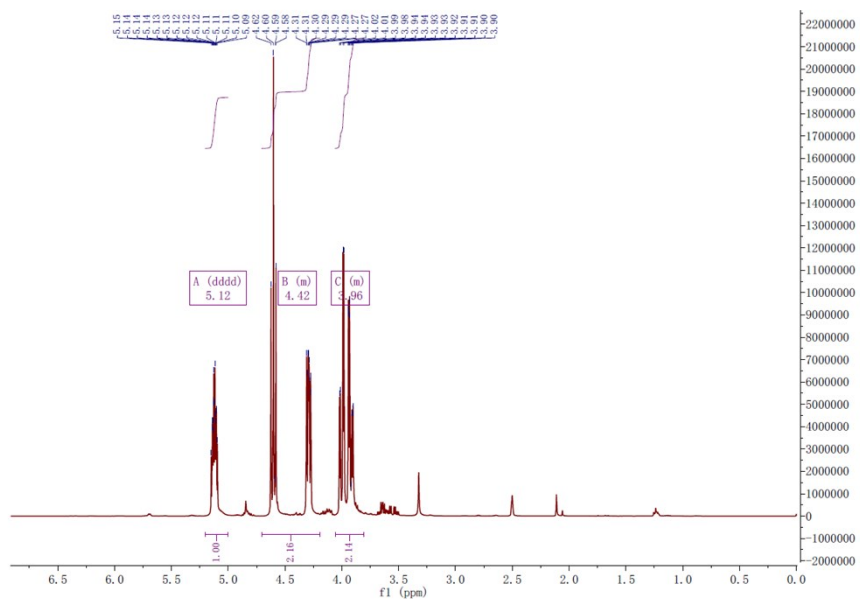


**Figure S42.**  $^1\text{H}$  NMR spectrum of 4-(chloromethyl)-1,3-dioxolan-2-one.

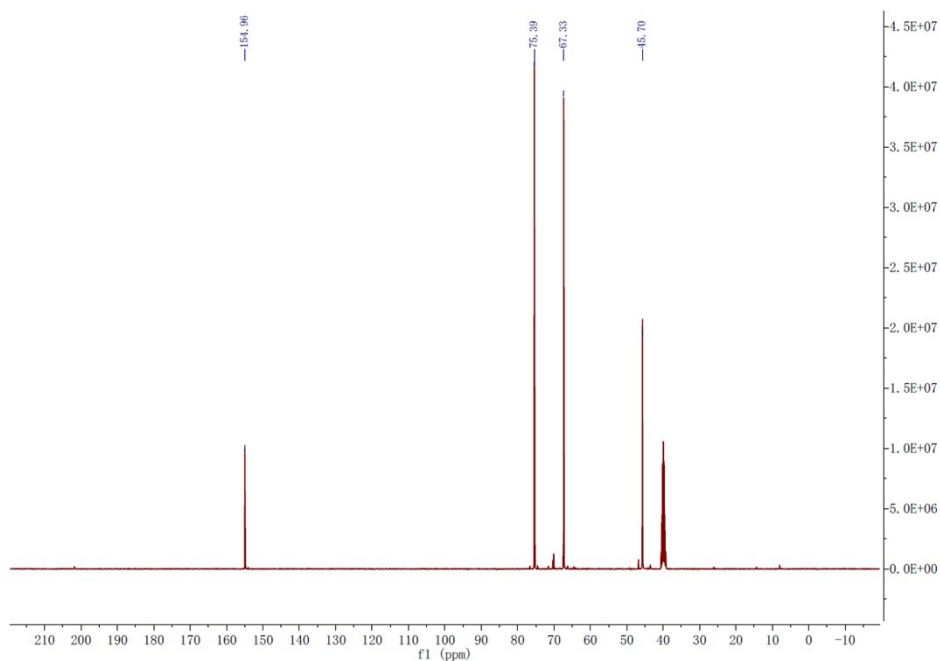
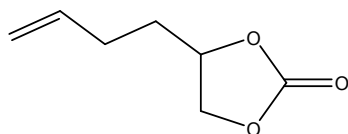


**Figure S43.**  $^{13}\text{C}$  NMR spectrum of 4-(chloromethyl)-1,3-dioxolan-2-one.





**4-(but-3-en-1-yl)-1,3-dioxolan-2-one**

$^1\text{H}$  NMR (400 MHz,  $\text{DMSO-}d_6$ )  $\delta$  5.82 (ddt,  $J = 16.9, 10.2, 6.6$  Hz, 1H), 5.08 (dq,  $J = 17.2, 1.7$  Hz, 1H), 5.00 (dq,  $J = 10.2, 1.4$  Hz, 1H), 4.78 (qd,  $J = 7.4, 5.4$  Hz, 1H), 4.56 (t,  $J = 8.1$  Hz, 1H), 4.15 (dd,  $J = 8.3, 7.1$  Hz, 1H), 2.21 – 2.03 (m, 2H), 1.87 – 1.71 (m, 2H).  $^{13}\text{C}$  NMR (101 MHz,  $\text{DMSO}$ )  $\delta$  155.28, 137.62, 116.03, 76.96, 69.57, 32.49, 28.71.

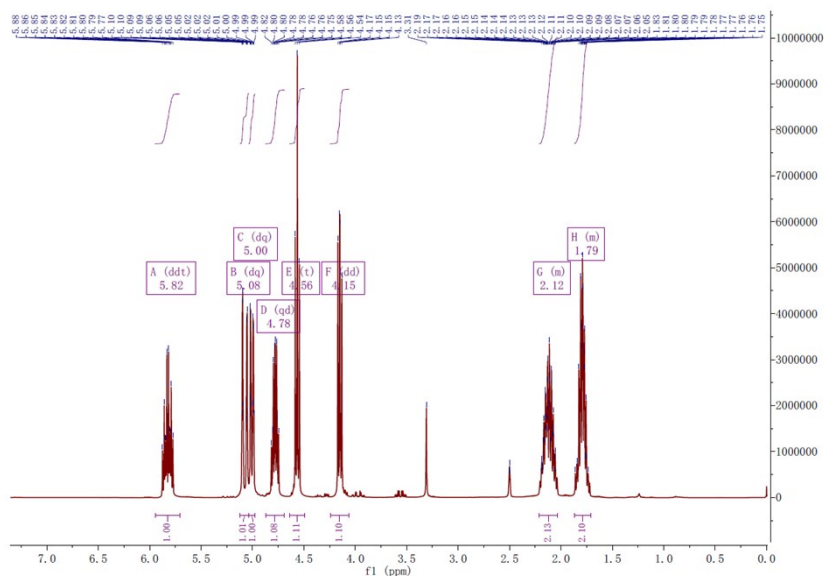


**Figure S44.**  $^1\text{H}$  NMR spectrum of 4-(but-3-en-1-yl)-1,3-dioxolan-2-one.

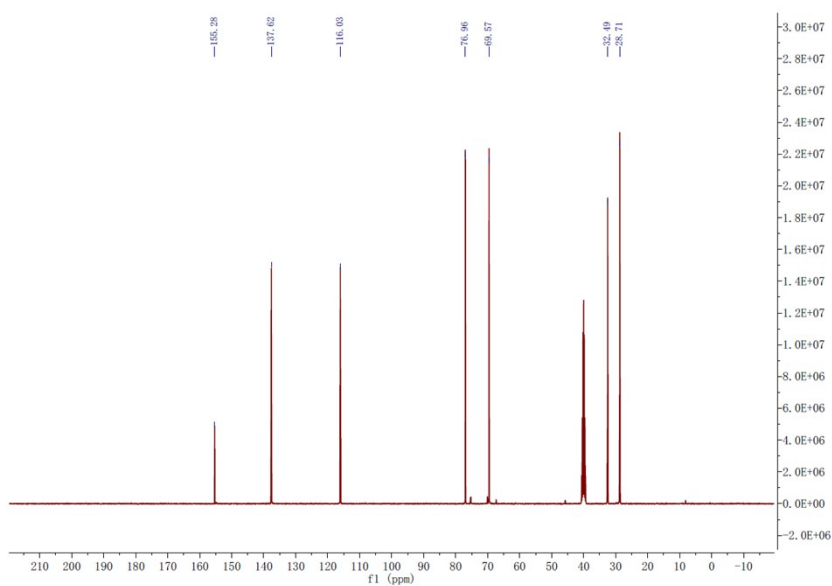
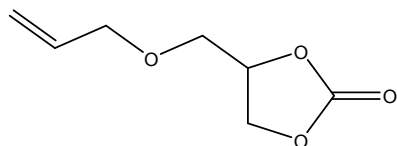


**Figure S45.**  $^{13}\text{C}$  NMR spectrum of 4-(but-3-en-1-yl)-1,3-dioxolan-2-one.



#### 4-((allyloxy)methyl)-1,3-dioxolan-2-one

$^1\text{H}$  NMR (400 MHz,  $\text{DMSO-}d_6$ )  $\delta$  5.88 (ddt,  $J = 17.2, 10.5, 5.3$  Hz, 1H), 5.26 (dq,  $J = 17.3, 1.8$  Hz, 1H), 5.17 (dq,  $J = 10.5, 1.6$  Hz, 1H), 4.94 (dddd,  $J = 8.5, 5.8, 4.1, 2.7$  Hz, 1H), 4.53 (t,  $J = 8.4$  Hz, 1H), 4.27 (dd,  $J = 8.3, 5.8$  Hz, 1H), 4.01 (dt,  $J = 5.3, 1.6$  Hz, 2H), 3.68 – 3.55 (m, 2H).  $^{13}\text{C}$  NMR (101 MHz,  $\text{DMSO}$ )  $\delta$  155.43, 135.10, 117.23, 75.95, 71.84, 69.58, 66.56.

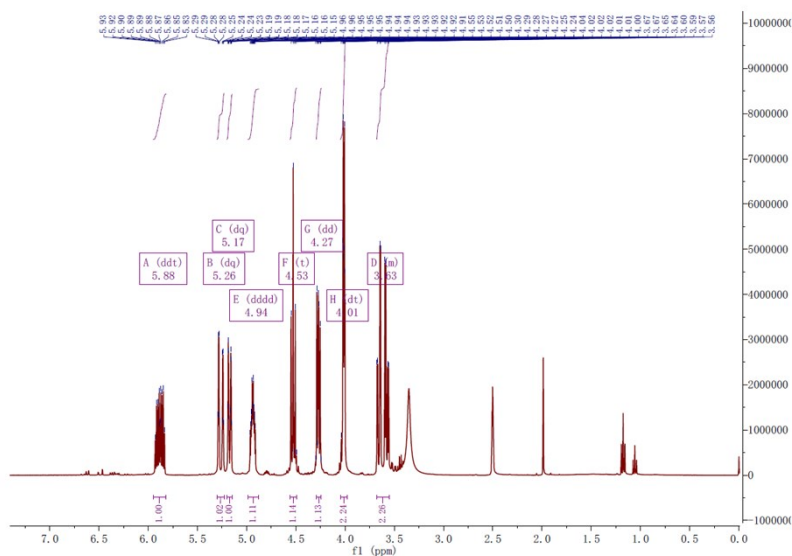


**Figure S46.**  $^1\text{H}$  NMR spectrum of 4-((allyloxy)methyl)-1,3-dioxolan-2-one.

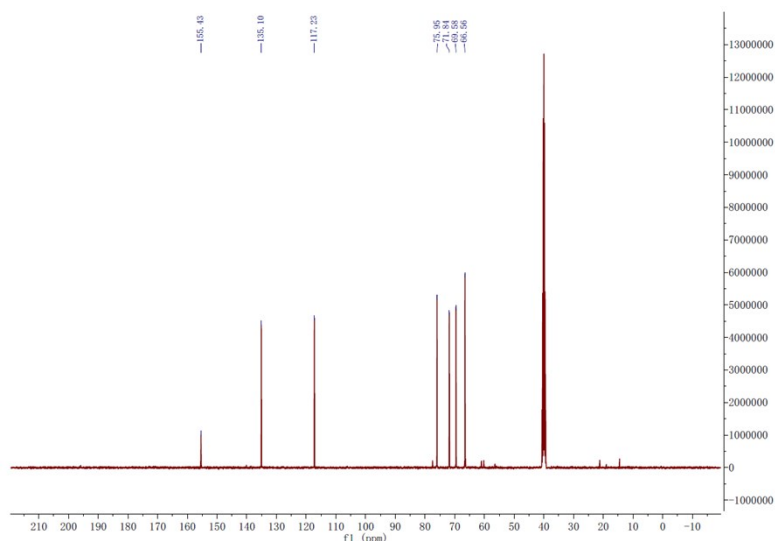
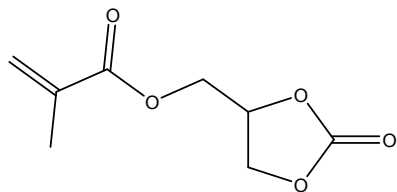


**Figure S47.**  $^{13}\text{C}$  NMR spectrum of 4-((allyloxy)methyl)-1,3-dioxolan-2-one.



**(2-oxo-1,3-dioxolan-4-yl)methyl methacrylate**

$^1\text{H}$  NMR (400 MHz,  $\text{DMSO-}d_6$ )  $\delta$  6.05 (t,  $J = 1.3$  Hz, 1H), 5.74 (p,  $J = 1.7$  Hz, 1H), 5.21 – 5.00 (m, 1H), 4.69 – 4.37 (m, 2H), 4.37 – 4.23 (m, 2H), 1.89 (d,  $J = 1.3$  Hz, 3H).

$^{13}\text{C}$  NMR (101 MHz,  $\text{DMSO}$ )  $\delta$  166.49, 155.22, 135.80, 126.98, 74.67, 66.66, 64.46, 18.25.

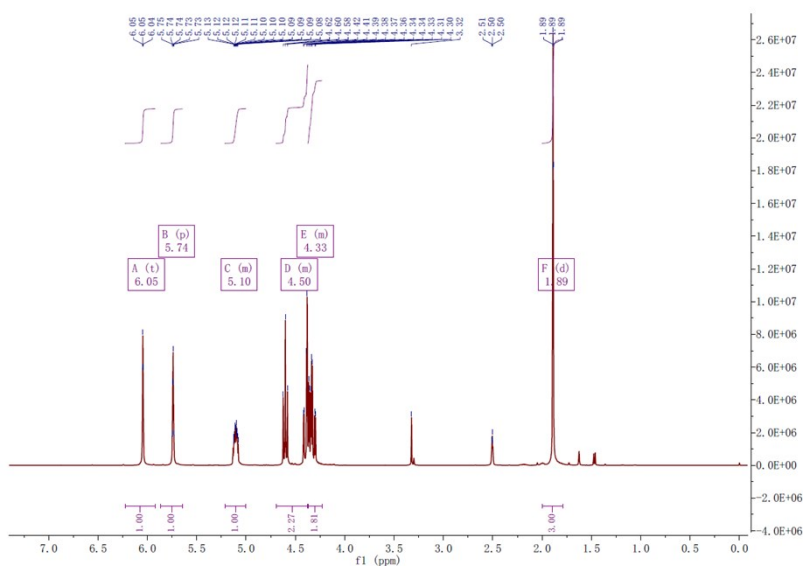


**Figure S48.**  $^1\text{H}$  NMR spectrum of (2-oxo-1,3-dioxolan-4-yl)methyl methacrylate.

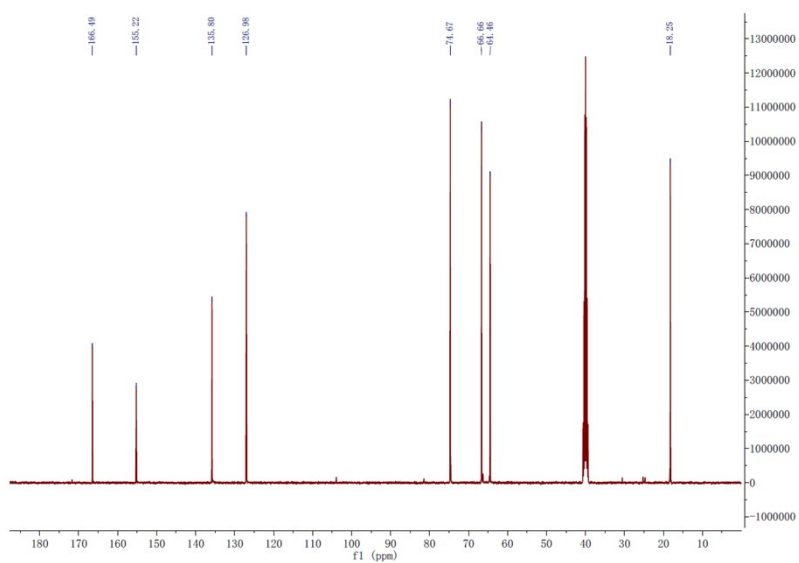
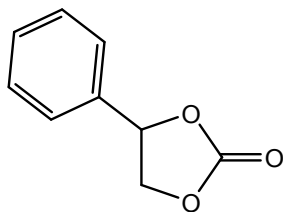


**Figure S49.**  $^{13}\text{C}$  NMR spectrum of (2-oxo-1,3-dioxolan-4-yl)methyl methacrylate.



**4-phenyl-1,3-dioxolan-2-one**

$^1\text{H}$  NMR (400 MHz,  $\text{DMSO-}d_6$ )  $\delta$  7.46 (tdd,  $J = 8.3, 5.8, 4.0$  Hz, 5H), 5.86 (t,  $J = 7.9$  Hz, 1H), 4.89 (t,  $J = 8.3$  Hz, 1H), 4.42 (t,  $J = 8.2$  Hz, 1H).  $^{13}\text{C}$  NMR (101 MHz, DMSO)  $\delta$  155.19, 136.76, 129.84, 129.38, 127.16, 78.24, 71.29.

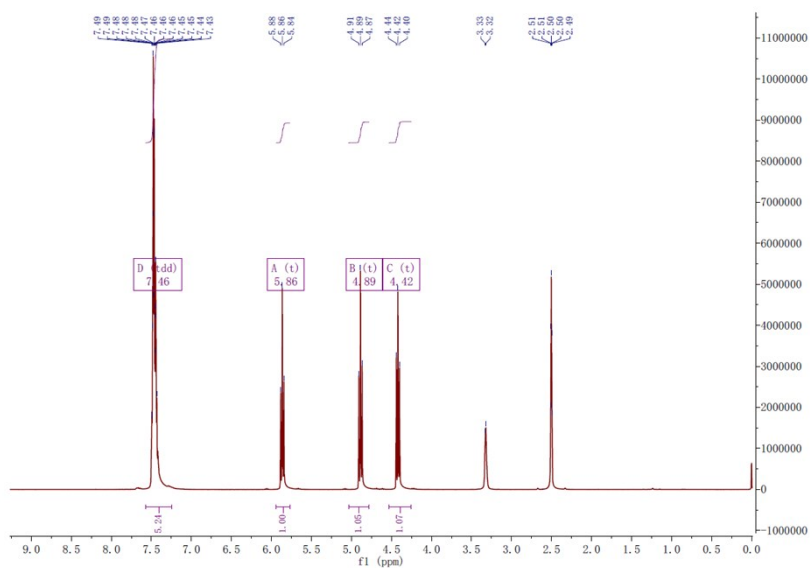


**Figure S50.**  $^1\text{H}$  NMR spectrum of 4-phenyl-1,3-dioxolan-2-one.

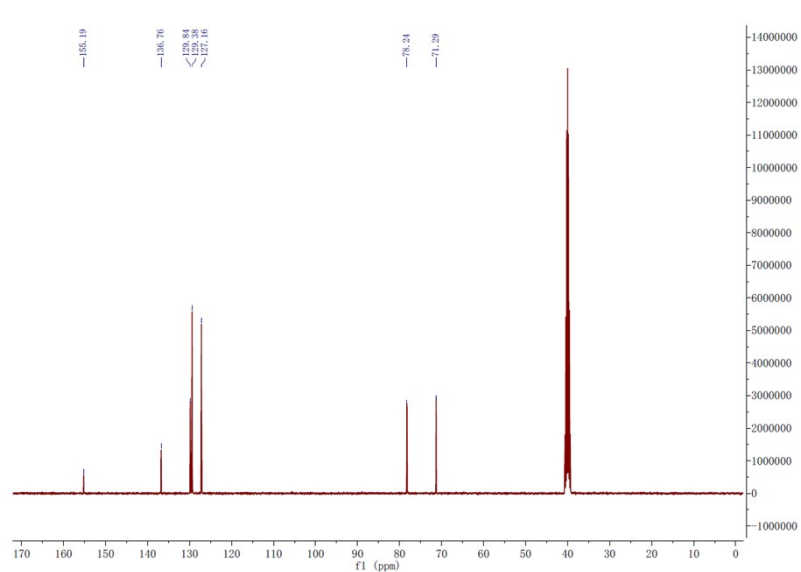
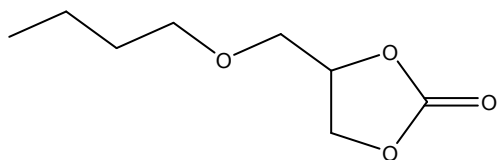


**Figure S51.**  $^{13}\text{C}$  NMR spectrum of 4-phenyl-1,3-dioxolan-2-one.



**4-(butoxymethyl)-1,3-dioxolan-2-one**

$^1\text{H}$  NMR (400 MHz,  $\text{DMSO-}d_6$ )  $\delta$  4.91 (dddd,  $J = 8.6, 5.9, 4.1, 2.7$  Hz, 1H), 4.60 – 4.18 (m, 2H), 3.69 – 3.51 (m, 2H), 3.45 (t,  $J = 6.5$  Hz, 2H), 1.58 – 1.41 (m, 2H), 1.32 (q,  $J = 7.4$  Hz, 2H), 0.88 (t,  $J = 7.4$  Hz, 3H).  $^{13}\text{C}$  NMR (101 MHz, DMSO)  $\delta$  155.40, 76.00, 71.01, 70.02, 66.51, 31.56, 19.14, 14.07.

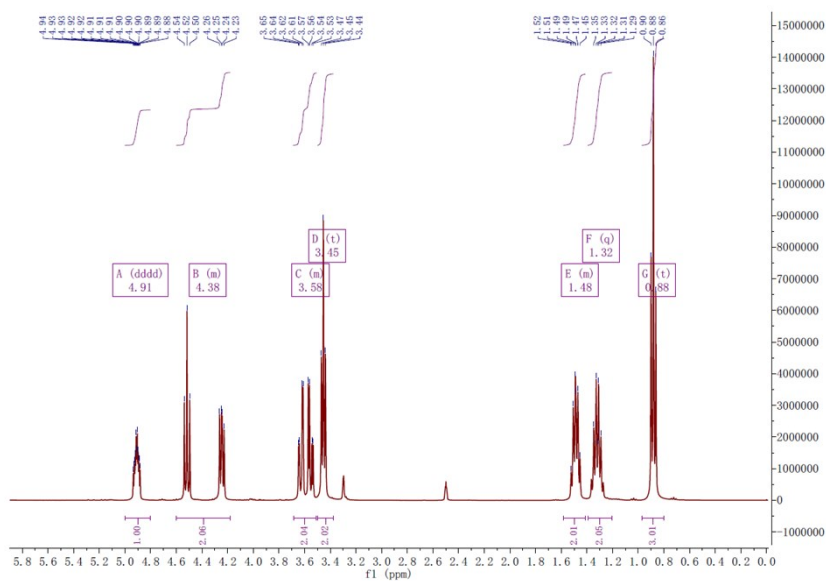


**Figure S52.**  $^1\text{H}$  NMR spectrum of 4-(butoxymethyl)-1,3-dioxolan-2-one.

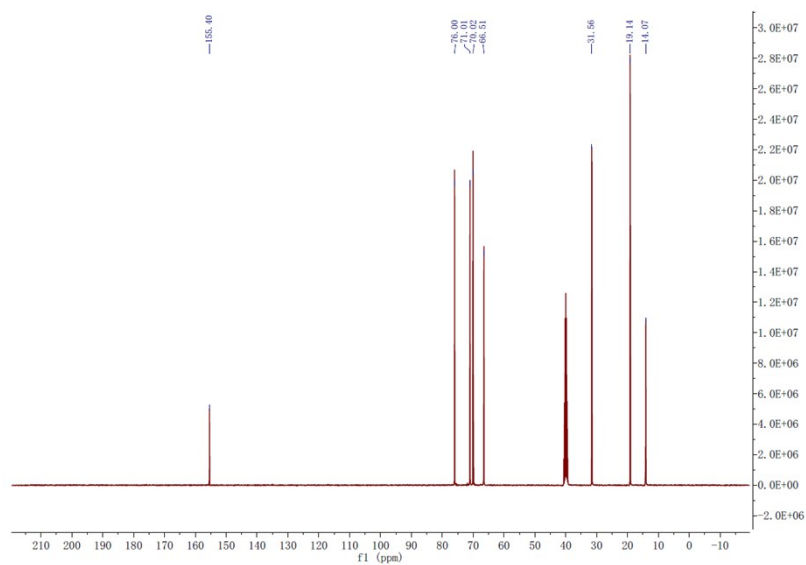
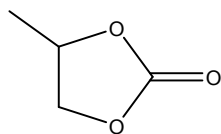
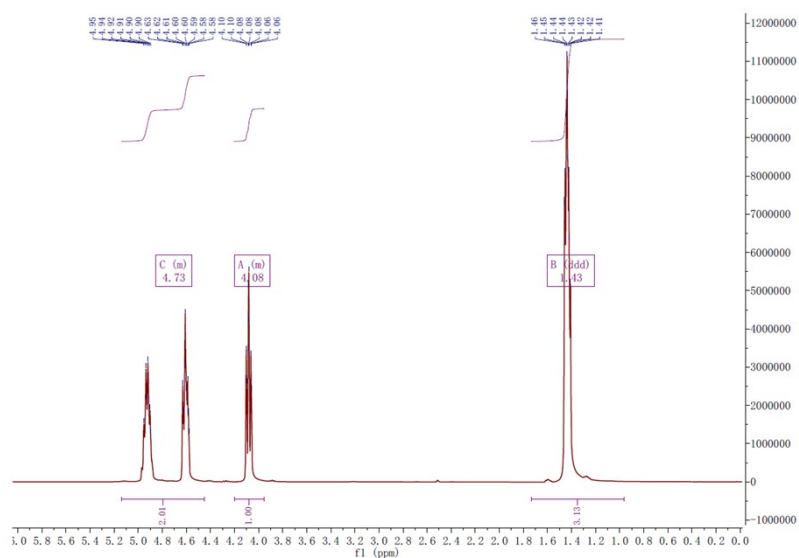


**Figure S53.**  $^{13}\text{C}$  NMR spectrum of 4-(butoxymethyl)-1,3-dioxolan-2-one.

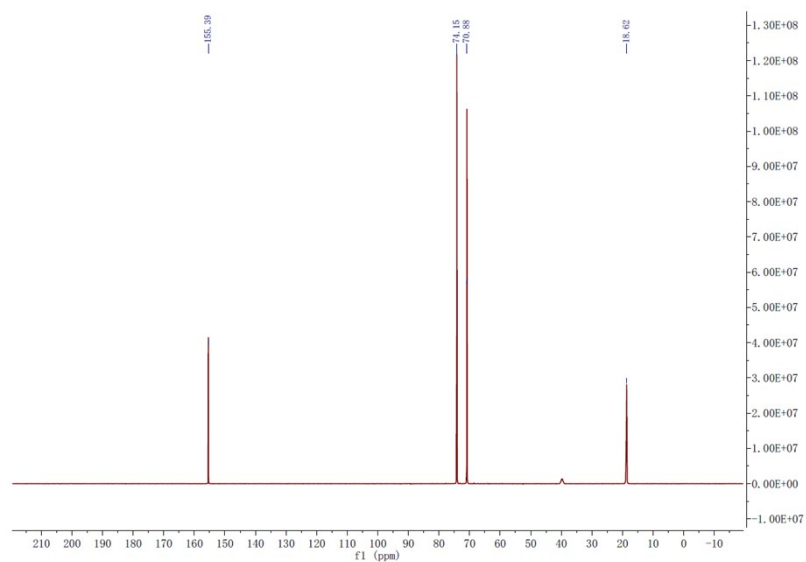


**4-methyl-1,3-dioxolan-2-one**

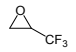
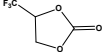
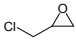
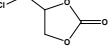
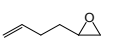
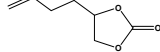
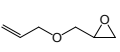
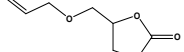
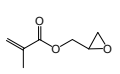
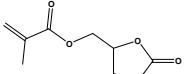
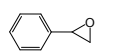
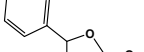
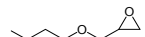

$^1\text{H}$  NMR (400 MHz,  $\text{DMSO-}d_6$ )  $\delta$  5.14 – 4.45 (m, 2H), 4.20 – 3.96 (m, 1H), 1.43 (ddd,  $J = 11.2, 6.1, 3.4$  Hz, 3H).  $^{13}\text{C}$  NMR (101 MHz,  $\text{DMSO}$ )  $\delta$  155.39, 74.15, 70.88, 18.62.



**Figure S54.**  $^1\text{H}$  NMR spectrum of 4-methyl-1,3-dioxolan-2-one.



**Figure S55.**  $^{13}\text{C}$  NMR spectrum of 4-methyl-1,3-dioxolan-2-one.

Entry	Substrate	Product	Yield <sup>a</sup> / %	TON <sup>b</sup>	TOF (h <sup>-1</sup> ) <sup>c</sup>
1			69.1	1665	555
2			62.1	1496	499
3			80.5	1938	655
4			83.5	2012	671
5			79.0	1708	569
6			82.0	1976	659
7			84.4	2034	678

<sup>a</sup> calculated based upon epoxide. <sup>b</sup>TON=[moles of product]/[(moles of MOP in MOP-alginate-SiO<sub>2</sub>)]. <sup>c</sup>TOF=TON/reaction time.

**Table S1.** Survey of substrate scope for the cycloaddition of epoxides with CO<sub>2</sub> over MOP-alginate-SiO<sub>2</sub>.

## Reference

1. E. Perez-Mayoral, Z. Musilova, B. Gil, B. Marszalek, M. Polozij, P. Nachtigall and J. Cejka, *Dalton Trans.*, 2012, **41**, 4036-4044.